Radiation Dosimetry of [82]Rb in Humans Under Pharmacologic Stress

Srinivasan Senthamizhchelvan[1], Paco E. Bravo[1], Martin A. Lodge[1], Jennifer Merrill[1], Frank M. Bengel[1,2], and George Sgouros[1]

[1]Division of Nuclear Medicine, Russell H. Morgan Department of Radiology and Radiological Science, Johns Hopkins University, Baltimore, Maryland; and [2]Department of Nuclear Medicine, Hannover Medical School, Hannover, Germany

[82]Rb is used with PET for cardiac perfusion studies. Using human biokinetic measurements, in vivo, we recently reported on the resting-state dosimetry of this agent. The objective of this study was to obtain [82]Rb dose estimates under stress. **Methods:** [82]Rb biokinetics were obtained in 10 healthy volunteers (5 male, 5 female; mean age ± SD, 33 ± 10 y; age range, 18–50 y) using whole-body PET/CT. The 76-s half-life of [82]Rb and the corresponding need for pharmacologic vasodilation require that all imaging be completed within 10 min. To accommodate these constraints, while acquiring the data needed for dosimetry we used the following protocol. First, a whole-body attenuation correction CT scan was obtained. Then, a series of 3 whole-body PET scans was acquired after a single infusion of 1.53 ± 0.12 GBq of [82]Rb at rest. Four minutes after the infusion of a 0.56 mg/kg dose of the vasodilator, dipyridamole, 3 serial whole-body PET scans were acquired after a single infusion of 1.50 ± 0.16 GBq of [82]Rb under stress. The time-integrated activity coefficient (TIAC) for stress was obtained by scaling the mean rest TIAC obtained from our previous rest study by the stress-to-rest TIAC ratio obtained from the rest–stress measurements described in this report. **Results:** The highest mean organ-absorbed doses under stress were as follows: heart wall, 5.1, kidneys, 5.0, lungs, 2.8, and pancreas, 2.4 μGy/MBq (19, 19, 10.4, and 8.9 mrad/mCi, respectively). The mean effective doses under stress were 1.14 ± 0.10 and 1.28 ± 0.10 μSv/MBq using the tissue-weighting factors of the International Commission on Radiological Protection, publications 60 and 103, respectively. **Conclusion:** Appreciable differences in source-organ biokinetics were observed for heart wall and kidneys during stress when compared with the previously reported rest study. The organ receiving the highest dose during stress was the heart wall. The mean effective dose calculated during stress was not significantly different from that obtained at rest.

Key Words: myocardium; [82]Rb; dipyridamole; stress dosimetry

Medical imaging procedures using ionizing radiation are steadily increasing. Cardiac imaging procedures for evaluation of cardiovascular conditions represent an important source of radiation exposure in the United States. Myocardial perfusion imaging contributes about 22% of the total effective dose (ED) from general medical imaging (*1*). PET is increasingly used for myocardial perfusion imaging and is gaining wide acceptance in the nuclear cardiology community. In a recent publication, we used human biokinetic data to calculate the dosimetry of the clinical PET perfusion tracer [82]Rb in subjects at rest (*2*). In that report, we addressed the significant differences that exist between dose estimates given in the package insert of the CardioGen-82 generator (Bracco Diagnostics Inc.) and a publication of the International Commission on Radiological Protection (ICRP) (*3*).

Myocardial PET perfusion imaging with [82]Rb is generally performed under both rest and stress conditions. Most stress imaging is performed using pharmacologic stress agents because of the short half-life of [82]Rb. The hemodynamics, biokinetics, and absorbed doses of organs during stress are expected to be different from those during rest. In this report, we present [82]Rb dosimetry for subjects under pharmacologic stress.

MATERIALS AND METHODS

Subjects

Ten healthy volunteers (5 male, 5 female; mean age ± SD, 33 ± 10 y; age range, 18–50 y) were included in this study; subject details are given in Table 1. All volunteers were prescreened before inclusion in the study. Medical history was taken, concurrent medications assessed, physical examination performed, vital signs checked, 12-lead electrocardiography performed, and blood and urine sampled to check for hematologic and clinical pathologic abnormalities and for substance abuse. Anyone with evidence of clinical disease, a history of organ-removal surgery (e.g., cholecystectomy, hysterectomy, or splenectomy), or a history of substance abuse was excluded. In women, pregnancy was ruled out. Volunteers were asked not to consume xanthines (e.g., caffeine or aminophylline) for at least 12 h before the test because these agents directly block the effects of adenosine and dipyridamole. The protocol was approved by the Johns Hopkins

TABLE 1
Research Subject Characteristics

Subject no.	Age (y)	Sex	Mass (kg)	Height (m)	Body mass index (kg/m²)	Administered activity of ^{82}Rb (MBq)	
						Rest	Stress
RB011	32	M	61	1.65	22.4	1,523	1,212*
RB012	39	F	62	1.60	24.2	1,588	1,595
RB013	18	M	76	1.73	25.4	1,634	1,594
RB014	42	M	68	1.57	27.6	1,331	1,335
RB015	31	F	57	1.55	23.7	1,556	1,544
RB016	29	M	71	1.68	25.2	1,747	1,777
RB017	18	M	64	1.63	24.1	1,529	1,533
RB018	42	F	75	1.55	31.2	1,395	1,395
RB019	50	F	67	1.60	26.2	1,573	1,570
RB020	31	F	69	1.78	21.8	1,463	1,463
Mean ± SD	33.2 ± 10.3		67 ± 6.1	1.63 ± 0.1	25.2 ± 3	1,534 ± 118	1,502 ± 158

*Infusion terminated abruptly because of high pressure in infusion line.

Institutional Review Board. All volunteers gave written informed consent.

^{82}Sr/^{82}Rb Generator

The commercially available ^{82}Sr/^{82}Rb generator, CardioGen-82, was used to elute ^{82}Rb activity. Details of the quality control procedures for the generator and cross calibration of end-of-infusion activity between the generator and the PET/CT scanner are described elsewhere (2).

PET/CT

All ^{82}Rb PET/CT (Discovery Rx; GE Healthcare) acquisitions were performed in 2-dimensional mode. The 76.38-s half-life of ^{82}Rb and the corresponding requirement for pharmacologic vasodilation require that image acquisition be completed within 10 min of the ^{82}Rb infusion. The following protocol was used to collect the pharmacokinetic data needed for dosimetry while remaining within the required constraints. First, a whole-body transmission CT scan (120 kVp; 20–200 mA, automatically adjusted; pitch, 0.5; and rotation time, 0.5 s) was obtained. A series of 3 whole-body PET scans was subsequently acquired after an infusion of 1,534 ± 118 MBq of ^{82}Rb at rest. Stress was induced by administration of the vasodilator, dipyridamole. Four minutes after a 4-min infusion of dipyridamole (0.56 mg/kg), about 1,502 ± 158 MBq of ^{82}Rb were infused and 3 serial whole-body PET scans were acquired. The heart rate, blood pressure, and electrocardiogram were monitored continuously throughout pharmacologic vasodilation. Each whole-body PET scan was obtained with a maximum of six 20-s bed positions starting at the level of the femurs and extending to the base of the skull. The 3 serially collected whole-body PET scans were completed in approximately 9 min. The mean infusion time for the ^{82}Rb activity from the ^{82}Sr/^{82}Rb generator was 25 s (range, 18–32 s). The first scan was started from the base of the femurs 10 s after the end of ^{82}Rb infusion. Attenuation-corrected whole-body PET images were reconstructed for subsequent region-of-interest analysis.

Source-Organ Contouring

All PET/CT images were transferred into MIMvista image analysis software (version 4.2; MIMvista Corp.). The source organs were delineated on the CT images with the help of fused PET/CT images. Except for muscle, thymus, and bone (cortical and trabecular), all the source organs expected for dose estimation were delineated. The gastrointestinal tract source organs were delineated into 4 regions: stomach contents, small intestine contents, upper large intestine (ascending and transverse colon) contents, and lower large intestine (descending and sigmoid colon) contents. The contour for heart contents (blood pool in cavities) was obtained using the difference between contours drawn for the whole heart and those drawn for the heart wall (visualized ventricular myocardium). Red bone marrow was delineated on the femur bone. Each bed position in the whole-body PET scan had a different factor applied for decay correction. To obtain the uncorrected counts (Bq/cm³) for each source organ at each time point, the source-organ contours that spanned more than 1 bed position were split into 2 or more contours according to their bed positions in the whole-body PET scan.

Dosimetry

The MIRD Committee schema (4) as implemented in the OLINDA/EXM 1.0 software (5) was used to perform the absorbed dose calculations. The time-integrated activity coefficient (TIAC) (or residence time) is required as input for these calculations. This coefficient is obtained by integrating the time-dependent activity curve for each source tissue. The ultra-short half-life of ^{82}Rb poses a challenge for obtaining such curves over the whole body. Usually, with longer-lived tracers dosimetry studies use serial whole-body images for measurement of organ uptake and clearance. The rapid decay of ^{82}Rb precludes imaging for more than 10 min after a single administration of activity and thus limits the number and count statistics of serial whole-body images. A maximum of 3 serial whole-body images could be obtained while maintaining adequate count statistics. A repeated-injection protocol as used in our previous study (2) could not be implemented because the imaging time would have exceeded the duration of pharmacologic vasodilation. Therefore, to obtain the pharmacokinetic data for dosimetry calculations under stress conditions, we used the 3-time-point whole-body rest–stress PET scans to obtain a ratio of stress to rest TIAC. This ratio was used to scale the mean TIAC obtained from the multibed multiinjection method used in the rest-only studies (2). The validity of this methodology was checked by

comparing the TIAC obtained at rest from the 3-time-point study with that obtained from the detailed biokinetics (rest) study (*2*).

This approach was implemented as follows. Contours delineated on whole-body CT as described earlier in the section on source-organ contouring were overlaid onto each whole-body rest–stress PET image to extract activity concentrations. Organ volumes from CT were converted to mass using published density values (*6,7*). The mass of organ contents was obtained by multiplying the volume by the CT-measured average density. Decay corrections applied during image reconstructions were reversed using decay factors from image headers. The administered activities (A_0) listed in Table 1 were the end-of-infusion values obtained from the ^{82}Rb generator, after correcting for the cross-calibration factor between the PET/CT and the ^{82}Rb generator output as described previously (*2*). For each source organ (r_S), a monoexponential expression was fit to the time-dependent activity curves (3 time points) obtained from the matched whole-body rest–stress (RS) studies. The fitted expressions were analytically integrated to give the time-integrated activity (TIA) for rest (R) and also for stress (S), (designated $\tilde{A}_{R,RS}(r_S)$ and $\tilde{A}_{S,RS}(r_S)$, respectively). These values were divided by the administered activity to give the TIAC (analogous to residence time and designated $\tilde{a}_{R,RS}(r_S)$ and $\tilde{a}_{S,RS}(r_S)$, respectively). The ratio of stress to rest TIAC was used to scale the mean rest TIAC concentration ($[\tilde{a}_R(r_S)]$) obtained from the previously reported rest-only study for which we had detailed pharmacokinetic data (*2*). The resulting scaled rest-only TIAC concentration was set equal to the stress TIAC concentration used in the dosimetry calculations. This approach assumes that the administered activity–normalized stress-to-rest ratio observed at the 3 measured time points applies to all time points for all organs and that the shape of the mean normalized rest time–activity curve obtained from the previous study (*2*) is representative of all normalized rest curves. The expression for obtaining the stress TIAC concentration ($[\tilde{a}_S(r_S)]$) is shown below:

$$[\tilde{a}_S(r_S)] = [\tilde{a}_R(r_S)] \cdot \frac{\tilde{a}_{S,RS}(r_S)}{\tilde{a}_{R,RS}(r_S)}. \qquad \text{Eq. 1}$$

To confirm that scaling in this manner is reasonable, we compared the TIAC concentration obtained from the rest curve of the 3-time-point rest–stress study, $\tilde{a}_{R,RS}(r_S)$, with that obtained from the previous rest-only study, $[\tilde{a}_R(r_S)]$. Because it was not possible to resolve the rising portion of the time-dependent activity curve in the 3-time-point rest–stress study, we corrected for this factor as shown in Equation 2 before making the comparison. The correction essentially replaces the back-extrapolated portion of the RS curve with the rising portion obtained from the mean rest-only time-dependent activity curve:

$$[\tilde{a}'_{R,RS}(r_S)] = \int_0^\infty [a_{R,RS}(r_S,t)] - \int_0^T [a_{R,RS}(r_S,t)]$$
$$+ \int_0^T [a_R(r_S,t)]. \qquad \text{Eq. 2}$$

The first integral in Equation 2 is $[\tilde{a}_{R,RS}(r_S)]$; the last integral is calculated by the trapezoidal method. A graphical illustration of Equation 2 is shown in Figure 1.

For each subject, the TIAC concentrations obtained from Equation 1 were multiplied by the standard source-organ mass and were input into OLINDA/EXM 1.0 (*5*) for dose estimation.

Because no activity was excreted by the subjects during imaging, the TIAC for the remainder of the body was calculated by subtracting the sum of the TIAC of all source organs from the reciprocal of the ^{82}Rb physical decay constant.

^{82}Rb activity observed in the gastrointestinal tract source organs (stomach, small intestine, upper large intestine, and lower large intestine) is due to blood flow to these organ walls. OLINDA/EXM 1.0 calculates the gastrointestinal tract (stomach, small intestine, upper large intestine, and lower large intestine) wall doses by assuming that the activity is in the contents. Therefore, we corrected the OLINDA/EXM 1.0 dose estimates for gastrointestinal tract walls so that the estimates corresponded to wall self-absorbed doses and not absorbed doses from contents to the wall. The correction was implemented as described previously (*2*).

RESULTS

Biokinetics

The mean ratio of stress to rest TIAC in source organs calculated using 3 measured time points from the whole-body rest–stress PET scan is given in Table 2. The ratio was less than 1 for kidneys, spleen, thyroid, ovaries, pancreas, lungs, brain, and adrenals and more than 1 for the remaining source organs. Notable differences in the ratios were observed for heart wall (1.37) and kidneys (0.86). Coronary vasodilators (adenosine and dipyridamole) exert their action by stimulating increases in coronary blood flow within the myocardium to maximal or near-maximal levels. The renal vasculature is also constricted during stress, which would explain lower blood flow to the kidneys during stress than at rest. Dipyridamole also induces dilatation of the splanchnic vasculature, resulting in a higher concentration of radiopharmaceuticals in the liver and intestinal tract during stress.

Given the current PET sensitivity, the short half-life of ^{82}Rb, and the limited stress period resulting from injected vasodilator pharmacodynamics, it is not possible to collect the number of whole-body PET scans required to adequately describe the pharmacokinetics of ^{82}Rb for dosimetry in stressed patients. Accordingly, the ratio of stress to rest TIAC obtained for each source organ in each subject was used to scale the previously known mean rest TIAC concentration. The mean TIAC during stress calculated across subjects is also listed in Table 2. The source organs with the highest mean TIAC (in seconds) were the lungs (10.2), liver (6.8), kidneys (6.0), heart content (5.2), and heart wall (3.9). For subject RB011, the third whole-body PET image after stress was count-poor because of a suboptimal ^{82}Rb activity infusion and was excluded from data analysis.

The validity of obtaining the stress TIAC by the above-described method was checked by comparing the mean TIAC at rest calculated from the 3-time-point whole-body PET scans (current study) with the multibed multiple-time-point PET protocol of the rest-only study (*2*). Figure 2 shows this comparison for selected source organs. The TIAC calculated using 3 time points was in general lower but comparable to that of the multibed, multiple-time-point method. The lungs exhibited the rapid uptake kinetics of
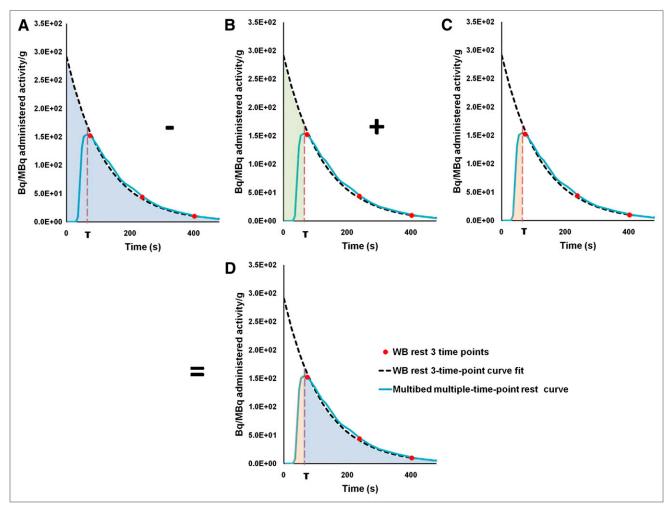
FIGURE 1. Graphical representation of Equation 2. Shaded regions in A, B, C, and D show $\int_0^\infty [a_{R,RS}(r_S,t)]$, $\int_0^T [a_{R,RS}(r_S,t)]$, $\int_0^T [a_R(r_S,t)]$, and $[\tilde{a}'_{R,RS}(r_S)]$, respectively, where T represents peak uptake time.

[82]Rb, which could not be calculated accurately using 3 time points—hence the higher differences as seen in Figure 2.

Organ-Absorbed Dose

The mean target organ–absorbed doses during stress across subjects are listed in Table 3. The organs with the highest mean absorbed dose per unit administered activity (μGy/MBq) were the heart wall (5.1), kidneys (5.0), lungs (2.8), pancreas (2.4), and stomach wall (2.2). The absorbed dose to tissues listed in Table 3 that were not assigned a TIAC reflects cross-fire photon contribution from organs that were assigned a TIAC as well as contribution from activity assigned to the remainder of the body.

A comparison of the radiation dose estimates for [82]Rb during stress obtained from this study with that during rest from the rest-only study (2) is shown in Figure 3. The main differences were in the organs with the highest absorbed dose per unit administered activity, which were the heart wall during stress and kidneys at rest. The absorbed dose to kidneys, thyroid, and spleen was lower—and the dose to the heart wall, intestine wall, and liver higher—during stress than at rest.

Effective Dose (ED)

The ED was calculated for each subject. The mean ED across subjects calculated by OLINDA/EXM 1.0, and based on ICRP 60 (8) tissue-weighting factors, was 1.14 ± 0.10 μSv/MBq. Using ICRP 103 tissue-weighting factors (9) and adjusting for tissues not listed in the OLINDA output, as described previously (2), a mean ED of 1.28 ± 0.10 μSv/MBq was obtained.

DISCUSSION

Most diagnostic nuclear cardiology studies involve imaging patients during 2 physiologic conditions: rest and stress. It is expected that the biokinetics of the radiotracer in various organs would differ during these 2 physiologic conditions, resulting in different absorbed doses and EDs. With the exception of ^{99m}Tc-labeled tracers (10), dose coefficients and EDs for rest and stress imaging are not generally available.

Pharmacologic agents (e.g., adenosine and dipyridamole) are routinely used in [82]Rb stress myocardial perfusion imaging. These agents are coronary vasodilators and exert

TABLE 2
Ratio of Stress to Rest TIAC from 3-Time-Point Whole-Body Rest–Stress PET Acquisition and Calculated
Stress TIAC Used in Dosimetry Calculations

Source organ	Stress–rest TIAC ratio (mean ± SD) (n = 9)	Stress TIAC (h) (mean ± SD) (n = 9)
Adrenals	9.38E–01 ± 1.77E–01	3.54E–05 ± 6.68E–06
Brain	9.42E–01 ± 2.80E–01	1.70E–04 ± 5.05E–05
Breasts	1.04E+00 ± 1.25E–01	5.03E–05 ± 6.06E–06
Gallbladder contents	1.13E+00 ± 3.10E–01	6.21E–05 ± 1.70E–05
Lower large intestine contents	1.37E+00 ± 4.40E–01	8.63E–05 ± 2.77E–05
Small intestine contents	1.13E+00 ± 1.53E–01	8.36E–04 ± 1.13E–04
Stomach contents	1.10E+00 ± 2.47E–01	3.98E–04 ± 8.89E–05
Upper large intestine contents	1.13E+00 ± 1.80E–01	2.67E–04 ± 4.24E–05
Heart contents	1.19E+00 ± 1.14E–01	1.44E–03 ± 1.39E–04
Heart wall	1.37E+00 ± 2.27E–01	1.09E–03 ± 1.80E–04
Kidneys	8.61E–01 ± 1.04E–01	1.68E–03 ± 2.03E–04
Liver	1.10E+00 ± 2.15E–01	1.89E–03 ± 3.71E–04
Lungs	9.50E–01 ± 1.25E–01	2.85E–03 ± 3.74E–04
Ovaries	8.19E–01 ± 6.00E–01	3.67E–06 ± 8.50E–07
Pancreas	9.37E–01 ± 1.57E–01	2.45E–04 ± 4.10E–05
Red marrow	1.58E+00 ± 8.69E–01	1.69E–04 ± 9.32E–05
Spleen	8.48E–01 ± 1.46E–01	2.97E–04 ± 5.11E–05
Testes	1.65E+00 ± 4.35E–01	7.97E–06 ± 5.00E–06
Thyroid	8.38E–01 ± 3.09E–01	3.48E–05 ± 1.29E–05
Urinary bladder contents	1.23E+00 ± 6.34E–01	4.89E–05 ± 2.52E–05
Uterus	1.03E+00 ± 3.61E–01	8.84E–05 ± 3.09E–05
Reminder of body	Not applicable	1.89E–02 ± 1.19E–03

their action by stimulating increases in coronary blood flow within the myocardium to maximal or near-maximal levels (11,12). However, the increase in coronary blood flow due to pharmacologic stress does not translate into a linear increase in myocardial tracer concentration. The myocardial uptake of ^{82}Rb shows a leveling-off phenomenon at high flow rates because of a decrease in first-pass extraction (13). When dipyridamole is used as a stress-inducing agent,
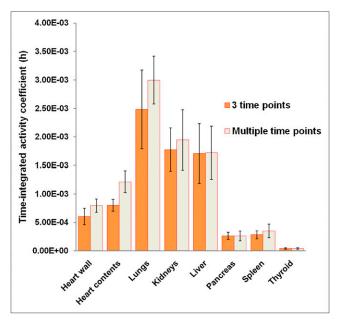

FIGURE 2. Comparison of mean TIAC (h) calculation at rest based on 3-time-point whole-body PET (current study) and multibed multiple-time-point PET (previous study (2)) for selected source organs.

the maximum effect occurs 3–7 min after completion of the 4-min infusion of dipyridamole. The hyperemic response is prolonged because the half-life of the drug is on the order of 30 min. This action of pharmacologic stress and the short half-life of ^{82}Rb make it impossible to obtain source-organ biokinetics using multiple-time-point whole-body imaging. Because of these constraints, it was necessary to obtain the input to the dosimetry calculations by scaling the source-organ TIAC values obtained from a rest-only study by the ratio of stress to rest TIAC.

The organ receiving the highest absorbed dose was the heart wall during stress, as compared with the kidneys at rest. Though differences in TIACs and corresponding differences in absorbed doses were observed between the stress study and the previous rest-only study (2), these differences were not significant except for heart wall. Comparison of source-organ TIAC at rest calculated using 3 whole-body PET images from this study with that calculated from the previous study (2) showed comparable results and supports our method. The mean ED (across subjects) calculated using ICRP 60 and ICRP 103 weighting factors during stress in this study was similar to that reported in our previous rest study (2).

In our previous report on ^{82}Rb dosimetry performed under resting conditions (2), we addressed the discrepancy in the prior dose estimates for ^{82}Rb between ICRP 53 (3) and the Cardiogen-82 package insert (14). Before our report on ^{82}Rb dosimetry, the 2 major sources of dose estimation were the ICRP 53 and the Radiation Internal Dose Information Center (RIDIC) compendium of dose estimates (15). The ICRP dose estimates were based on a flow model

TABLE 3
[82]Rb Absorbed Dose Estimates During Stress

Target organ	Absorbed dose (stress) (mGy/MBq) (mean ± SD) (n = 9)
Adrenals	1.99E–03 ± 3.73E–04
Brain	1.50E–04 ± 3.26E–05
Breasts	2.08E–04 ± 1.64E–05
Gallbladder wall	8.78E–04 ± 1.01E–04
Lower large intestine wall	8.43E–04 ± 7.26E–05
Small intestine	1.28E–03 ± 8.91E–05
Stomach wall	2.20E–03 ± 6.03E–04
Upper large intestine wall	1.82E–03 ± 4.17E–04
Heart wall	5.05E–03 ± 6.66E–04
Kidneys	5.02E–03 ± 6.25E–04
Liver	1.18E–03 ± 1.40E–04
Lungs	2.82E–03 ± 3.12E–04
Muscle	3.48E–04 ± 5.43E–05
Ovaries	3.94E–04 ± 6.32E–05
Pancreas	2.43E–03 ± 4.02E–04
Red marrow	3.32E–04 ± 2.84E–05
Osteogenic cells	5.11E–04 ± 9.03E–05
Skin	3.07E–04 ± 4.98E–05
Spleen	1.66E–03 ± 3.03E–04
Testes	2.59E–04 ± 5.29E–05
Thymus	4.07E–04 ± 5.42E–05
Thyroid	1.51E–03 ± 4.78E–04
Urinary bladder wall	4.44E–04 ± 5.29E–05
Uterus	1.02E–03 ± 4.36E–04
Total body	4.81E–04 ± 6.19E–05
Effective dose (mSv/MBq)*	1.28E–03 ± 9.58E–05

*Calculated using ICRP 103 tissue-weighting factors.

for the tracer, and the RIDIC dose estimates were based on human data for a limited number of source organs obtained using γ-camera imaging by Ryan et al. (16). Separate dose estimates for rest and stress conditions were not reported.
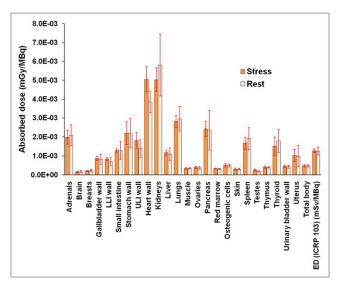

FIGURE 3. Comparison of absorbed dose estimates for [82]Rb at stress (current study) and at rest (previous study (2)).

Similar to our previous observations in the resting state dose estimation, the significant differences between our current stress dose estimation and the dose estimation reported in ICRP 53 were for thyroid and adrenals, which were 25- and 10-fold lower for our study than for ICRP 53. Also, the dose estimates for kidneys and lower large intestine wall were more than 3- and 4-fold lower for our study than for ICRP 53. As explained in our previous report, the conservative blood flow model adopted by the ICRP 53 is the major reason for the differences in dose estimation. On the other hand, the dose estimation by RIDIC using the data of Ryan et al. (16) was lower than our dose estimation overall.

When we compare our ED calculation based on ICRP 60 (8) weighting factors with the ICRP 53 data–derived ED (3.4E–03 mSv/MBq) as given in ICRP 80 (17), our ED for both rest and stress conditions is about 3-fold lower. However, the RIDIC-calculated ED is about 30% lower than our ED. Based on our previously reported dose estimation for [82]Rb at rest and the current dosimetry under pharmacologic stress, for a clinical [82]Rb PET scan with a 1,480-MBq injection at rest and stress (2 × 1,480 MBq) the total ED would be 3.3 mSv and 3.8 mSv based on ICRP 60 and ICRP 103 (9) weighting factors, respectively. For the same protocol, the organs receiving the highest equivalent doses would be the kidneys (16 mSv), heart wall (13 mSv), and lungs (9 mSv). The additional dose from a transmission CT scan for attenuation correction would need to be added (about 0.3 mSv for the cardiac region in our protocol) to obtain total ED from a clinical PET/CT procedure. The ED from CT strictly depends on the individual protocol, which may vary across institutions and scanners.

As the number of noninvasive cardiovascular imaging procedures continues to increase, the concern about increased radiation dose from these procedures has also grown (1,10). An effort is being made to use procedures with the lowest reasonably achievable radiation dose. Dosimetry for PET myocardial perfusion imaging tracers such as ^{13}N-ammonia and ^{15}O-water is well defined, and the resulting ED of clinical PET protocols with these tracers is substantially lower than that of SPECT protocols. The results obtained for [82]Rb under both rest (2) and stress conditions places it in the same lower dose range as alternative PET perfusion tracers.

CONCLUSION

The dose estimation under pharmacologic stress from this study, along with the previous dosimetry study performed at rest, provides comprehensive and detailed dosimetry for [82]Rb in humans. This information will help in decision making regarding risk–benefit analysis in cardiac test selection.

ACKNOWLEDGMENTS

REFERENCES

1. Fazel R, Krumholz HM, Wang Y, et al. Exposure to low-dose ionizing radiation from medical imaging procedures. *N Engl J Med.* 2009;361:849–857.

2. Senthamizhchelvan S, Bravo EP, Esaias C, et al. Human biodistribution and radiation dosimetry of ^{82}Rb. *J Nucl Med.* 2010;51:1592–1599.

3. International Commission on Radiological Protection (ICRP). *Radiation Dose to Patients from Radiopharmaceuticals*. ICRP Publication 53. New York, NY: Pergamon Press; 1988.

4. Bolch WE, Eckerman KF, Sgouros G, Thomas SR. MIRD pamphlet no. 21: a generalized schema for radiopharmaceutical dosimetry-standardization of nomenclature. *J Nucl Med.* 2009;50:477–484.

5. Stabin MG, Sparks RB, Crowe E. OLINDA/EXM: the second-generation personal computer software for internal dose assessment in nuclear medicine. *J Nucl Med.* 2005;46:1023–1027.

6. International Commission on Radiation Units and Measurements (ICRU). *Tissue Substitutes in Radiation Dosimetry and Measurement*. Bethesda, MD: ICRU; 1989. Report 44.

7. International Commission on Radiological Protection (ICRP). *Basic Anatomical and Physiological Data for Use in Radiological Protection: Reference Values*. Oxford, U.K.: Pergamon Press; 2002. ICRP Publication 89.

8. International Commission on Radiological Protection (ICRP). *1990 Recommendations of the International Commission on Radiological Protection*. New York, NY: Pergamon Press; 1991. ICRP Publication 60.

9. International Commission on Radiological Protection (ICRP). 2007 recommendations of the International Commission on Radiological Protection: ICRP publication 103. *Ann ICRP.* 2007;37:1–332.

10. Einstein AJ, Moser KW, Thompson RC, Cerqueira MD, Henzlova MJ. Radiation dose to patients from cardiac diagnostic imaging. *Circulation.* 2007;116:1290–1305.

11. Salcedo J, Kern MJ. Effects of caffeine and theophylline on coronary hyperemia induced by adenosine or dipyridamole. *Catheter Cardiovasc Interv.* 2009;74:598–605.

12. Heller GV, Calnon D, Dorbala S. Recent advances in cardiac PET and PET/CT myocardial perfusion imaging. *J Nucl Cardiol.* 2009;16:962–969.

13. Iskandrian AS, Verani MS, Heo J. Pharmacologic stress testing: mechanism of action, hemodynamic responses, and results in detection of coronary artery disease. *J Nucl Cardiol.* 1994;1:94–111.

14. CardioGen-82 [package insert]. Princeton, NJ: Bracco Diagnostics Inc.; 2000.

15. Stabin MG, Stubbs JB, Toohey RE. *Radiation Dose Estimates for Radiopharmaceuticals*. Washington, DC: U.S. Nuclear Regulatory Commission, U.S. Department of Energy, U.S. Department of Health and Human Services; 1996.

16. Ryan J, Harper P, Stark V, Peterson E, Lathrop K. Radiation absorbed dose estimate for Rb-82 using in vivo measurements in man [abstract]. *J Nucl Med.* 1984;25(suppl):94P.

17. International Commission on Radiological Protection (ICRP). *Radiation Dose to Patients from Radiopharmaceuticals*. Oxford, U.K.: Pergamon Press; 1999. ICRP Publication 80, Addendum 2 to ICRP Publication 53.